

## Analytical Investigation of the P- $\Delta$ Effect of Middle-rise Unbraced Steel Frames

Hee-Dong Kim<sup>1,\*</sup> and Myung-Jae Lee<sup>2</sup>

<sup>1</sup>Manager, Technical Sales Support Team, Hyundai Steel, Shinmonro 2-Ga, Jongro-gu, Seoul, 135-515, Korea

<sup>2</sup>Professor, Department of Architectural Engineering, Chung-Ang University, Heokseok-dong, Dongjak-gu, Seoul, 156-756, Korea

---

### Abstract

In this study, the influences of the P- $\Delta$  effect on the behavior of middle-rise unbraced steel frames and the validity of factor B2 were investigated using the analytical approach to suggest the basic design information on the P- $\Delta$  effect to the structural engineers. The refined plastic hinge method with an arc length algorithm was applied to the two-dimensional second-order inelastic analysis which can cover the post-maximum load behavior. Four types of middle-rise unbraced steel frames were selected as the subjects of the analysis. The main parameters of the analysis were the shape and the scale of the frame, the stiffness of the beam and the first-floor column, and the axial load ratio of the first-floor column. As revealed by the analytical research that was conducted, the P- $\Delta$  effect affects the behavior of middle-rise unbraced steel frames and the axial load, and the stiffness of the first-floor column are the main factors which govern the P- $\Delta$  effect. In addition, factor B2 is not applicable to the frame that has not clear story concept and it does not properly estimate the P- $\Delta$  effect of an unbraced frame when nonlinear-inelastic behavior is induced. Thus, reasonable guidelines are needed for the use of factor B2.

**Keywords:** P- $\Delta$  effect, factor B2, unbraced frame, 2-dimensional second-order inelastic analysis

---

### 1. Introduction

A large number of commercial buildings in downtown Korea are middle-rise steel frames because of the benefits of steel structures, such as fast construction and the effective use of materials (Kim, 2007).

The moment (rigid) frame system can be one of recommendation as the structural system for the abovementioned case (Figure 1), because this structural system is one of the most reliable ductile systems for lateral force resistance when special provisions are reasonably applied.

Moment frames are categorized as unbraced frames because they resist lateral forces through the flexural actions of the members that are framed into rigidly connected joints. In this case, lateral displacement ( $\Delta$ ) can be induced and it causes the P- $\Delta$  effect. This may seriously affect the stability of the unbraced frame (Galambos, 1968, 1998; Chen, 1991). Therefore, the P- $\Delta$  effect has to be properly considered during the design of unbraced frames.

---

Note.-Discussion open until February 1, 2011. This manuscript for this paper was submitted for review and possible publication on May 24, 2009; approved on July 28, 2010.

---

\*Corresponding author

Tel: +82-2-3464-4083; Fax: +82-2-3464-4087  
E-mail: drkimhd@hanafos.com

Since the early 1970s, studies have been undertaken to come up with a suitable method for considering the P- $\Delta$  effect. Most published studies about the P- $\Delta$  effect, however, focus on suggesting the moment amplification factor (Yura, 1971; Cheong-Siat-Moy, 1972; LeMessurier, 1972) or the second-order analysis method (Chen, 1991, 1995; Chan, 2000).

Because of this kind of background, very limited information, which can be used for the schematic design of unbraced frames, is available. In addition, it is hard for structural engineers to understand the limitation of all analysis method which can consider the P- $\Delta$  effect.

Therefore, the influence of the P- $\Delta$  effect on the behavior of middle-rise unbraced steel frames, the main factors which affect the P- $\Delta$  effect, and the limitation of analysis method which is used for considering the P- $\Delta$  effect should be investigated to suggest the basic information of the P- $\Delta$  effect to structural engineers.

For these purposes, the experimental study on the P- $\Delta$  effect was conducted by authors (Kim, 2001, 2002, 2009). The scale of the frame and the number of specimens were limited, though. Therefore, the analytical approach, the second-order inelastic analysis method was used to overcome the limitations of the experimental approach in this study.

The factor B2 method was selected in this study for the method which is expected to use for considering the P- $\Delta$  effect in design stage because it is recommended in KBC

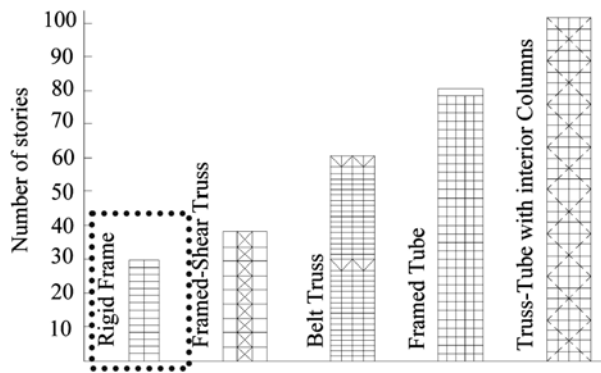


**Figure 1.** Classification of building structural systems by Fazlur Khan (Moon, 2007).

2009 (AIK, 2009) to consider the P- $\Delta$  effect of the unbraced steel frame with the first-order elastic analysis and it is more familiar with engineers than other methods.

## 2. Analytical Approach

### 2.1. Method of analysis

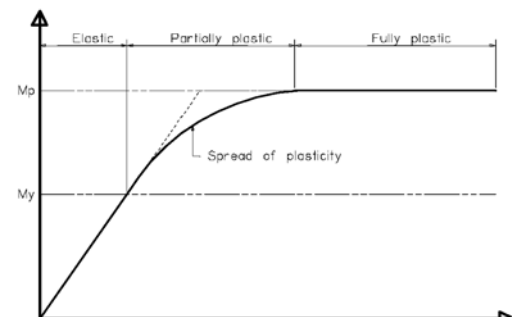
The second-order inelastic analysis is needed to investigate the P- $\Delta$  effect and factor B2, including for an inelastic region. Many analytical methods have been suggested for the second-order inelastic analysis and each of them has its own merits.

In this study, the refined plastic hinge method, which was suggested by W. F. Chen (1995) and S. E. Kim (1998), was used as the platform of analysis program because it has both reasonable accuracy and fast analysis speed.

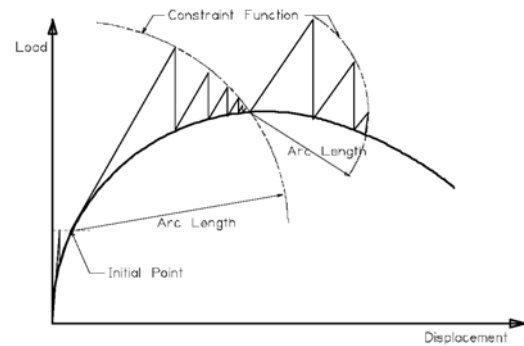
This method can consider the gradual yielding of the section with the moment-rotational angle model (Figure 2 (a)), the reduction of the full plastic moment of a section caused by the axial load, the reduction of the tangent modulus caused by the residual stress and the axial load, and second-order effects, such as the P- $\delta$  and P- $\Delta$  effects (Kim, 1998). Out of plane behaviors, such as lateral buckling or local buckling, were not considered in this method, though.

Most of the published refined plastic hinge method, however, adopted the Newton raphson method as the solving algorithm. Thus, the post-maximum load behavior could not be detected. The arc length method (Crisfield, 1983), which controls the load and the displacement at the same time with constrain function (Figure 2 (b)), was applied to improve solving algorithm (Kim, 2002) in this study. Thus, the influence of the P- $\Delta$  effect on the post-maximum load behavior was successfully investigated. The summarized conceptual diagrams of moment-rotational angle model and arc length method are shown in Figure 2.

To verify the program which is based on the refined plastic hinge method with arc length method, the analysis was conducted with the same parameters as those of the



(a) Moment-rotational angle model



(b) Arc length method

**Figure 2.** The conceptual diagrams of the program.

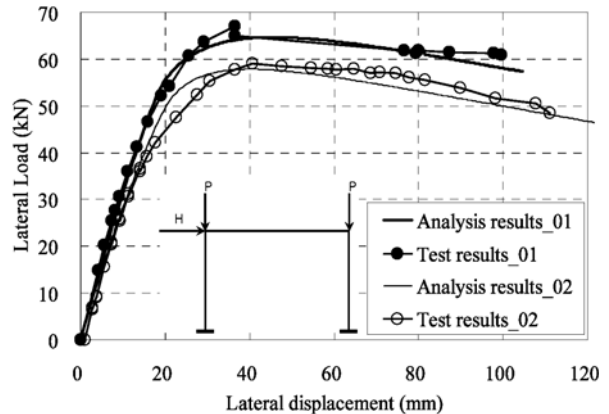


**Figure 3.** Comparison of the analysis results with the test results.

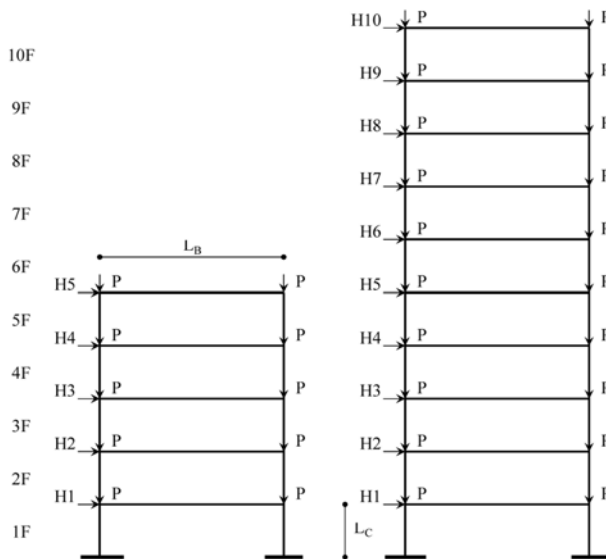
tests that the authors conducted (Kim, 2001, 2002, 2009). The specimens were one-story, one-span unbraced steel frames (See the picture in Figure 3), and the tests were conducted under static loading conditions.

The results of comparison are shown in Figure 3. The figure shows that the analysis results are consistent with the test results from the initial loading stage to the post-maximum loading stage. Therefore, it can be said that the analysis program is acceptable.

### 2.2. Second-order inelastic analysis

#### 2.2.1. Conditions of the analysis

For the analytical study, four types of middle-rise

**Figure 4.** Typical frames of analysis (1S cases).

unbraced steel frames-five-story, one-span (51 series); five-story, three-span (53 series); ten-story, one-span (101 series); and ten-story, three-span (103 series)-were selected.

The typical story height ( $L_C$ ) was 4,000 mm, and the typical span length ( $L_B$ ) was 12,000 mm. The boundary conditions were assumed as fixed, and all the connections of the beams to the columns were assumed as rigid. The design of the frames was based on KBC 2009, and the change in the member section was done per three-story unit for modeling convenience and considering the design practice.

Standard frames,  $L_C$  and  $L_B$ , and non-void series, were designed with strong-column, weak-beam conditions ( $M_{pc} > M_{pb}$ ), and the column stiffness was greater than the beam stiffness ( $I_c/L_c > I_b/L_b$ ). All of these conditions are commonly adopted as the design assumptions of commercial building.

The loads were calculated according to KBC 2009, and all the loads were applied on the nodes as nodal forces. To consider the real loading conditions of unbraced frames, the gravity loads were made constant from the start of the analysis to the end of it, but the lateral loads were varied. The pattern of the lateral loads depended on the seismic and wind load conditions.

### 2.2.2. Main parameters of the analysis

The main parameters of the analysis were the shape and the scale of the frame, the stiffness of the beam and the first-floor column, and the axial load ratio of the first-floor column.

The variation of the shape can cause the changes of the loading and the boundary conditions, and the scale of the frame is closely related to the loading conditions of it. The stiffness of the beam and column at the first-floor may govern the stiffness of the frame and it can affect the lateral displacement. The axial load ratio of the first-floor

**Table 1.** Parameters of the analysis

Case	Scale of frame	$L_C$ (mm)	$L_B$ (mm)	$I_c L_c / I_b L_b$	Axial load ratio	Void
51113N	5F/1S	4,000	12,000	1.55	0.3	×
51117N	5F/1S	4,000	12,000	1.55	0.7	×
51213N	5F/1S	8,000	12,000	0.78	0.3	×
51217N	5F/1S	8,000	12,000	0.78	0.7	×
51153N	5F/1S	4,000	6,000	0.78	0.3	×
51157N	5F/1S	4,000	6,000	0.78	0.7	×
53113N	5F/3S	4,000	12,000	1.55	0.3	×
53113E	5F/3S	4,000	12,000	1.55	0.3	○
53117N	5F/3S	4,000	12,000	1.55	0.7	×
53117E	5F/3S	4,000	12,000	1.55	0.7	○
53213N	5F/3S	8,000	12,000	0.78	0.3	×
53213E	5F/3S	8,000	12,000	0.78	0.3	○
53217N	5F/3S	8,000	12,000	0.78	0.7	×
53217E	5F/3S	8,000	12,000	0.78	0.7	○
53153N	5F/3S	4,000	6,000	0.78	0.3	×
53153E	5F/3S	4,000	6,000	0.78	0.3	○
53157N	5F/3S	4,000	6,000	0.78	0.7	×
53157E	5F/3S	4,000	6,000	0.78	0.7	○
101113N	10F/1S	4,000	12,000	1.66	0.3	×
101117N	10F/1S	4,000	12,000	1.66	0.7	×
101213N	10F/1S	8,000	12,000	0.83	0.3	×
101217N	10F/1S	8,000	12,000	0.83	0.7	×
101153N	10F/1S	4,000	6,000	0.83	0.3	×
101157N	10F/1S	4,000	6,000	0.83	0.7	×
103113N	10F/3S	4,000	12,000	1.66	0.3	×
103113E	10F/3S	4,000	12,000	1.66	0.3	○
103117N	10F/3S	4,000	12,000	1.66	0.7	×
103117E	10F/3S	4,000	12,000	1.66	0.7	○
103213N	10F/3S	8,000	12,000	0.83	0.3	×
103213E	10F/3S	8,000	12,000	0.83	0.3	○
103217N	10F/3S	8,000	12,000	0.83	0.7	×
103217E	10F/3S	8,000	12,000	0.83	0.7	○
103153N	10F/3S	4,000	6,000	0.83	0.3	×
103153E	10F/3S	4,000	6,000	0.83	0.3	○
103157N	10F/3S	4,000	6,000	0.83	0.7	×
103157E	10F/3S	4,000	6,000	0.83	0.7	○

\*  $M_{pc}/M_{pb}$ : 1.06 (5F), 1.38 (10F).

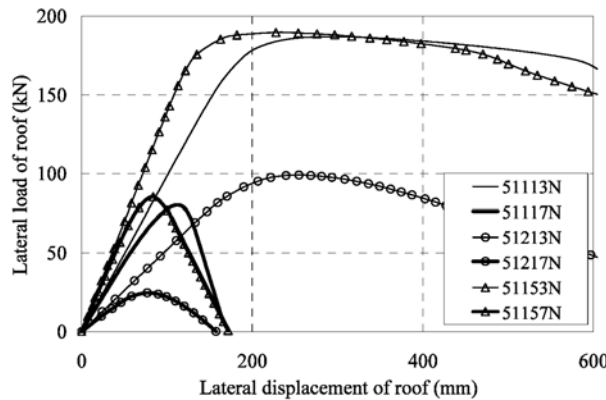
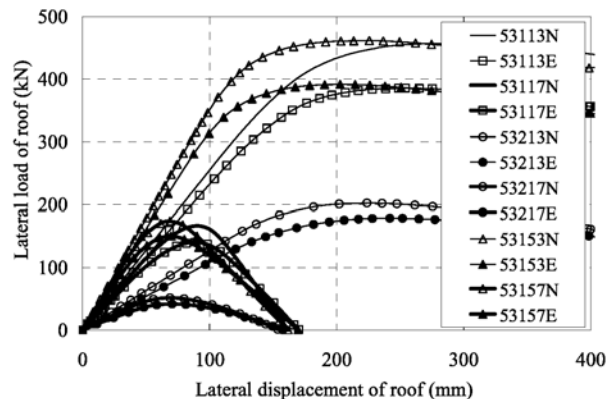
column is directly related to the P-Δ effect.

These parameters were selected based on preceding studies (Kim, 2001, 2002, 2009) and the values of parameters were set considering the common practice of structural design.

The main parameters of this study are summarized in Table 1. In this table, F refers to the floor; S, to the span; subscript C, to the column; and subscript B, to the beam. The axial load ratio is  $\Sigma P/P_y$  of the first-floor column. The quantity of the gravity nodal loads is based on the axial load ratio of each case. “Void” means the right-side beam

**Table 2.** Rule of the case name (103217E)

10	3	2	1	7	E
Story	Span	$L_C$	$L_B$	$P/P_y$	Void
5: 5F	1: 1S	1: $L_C$	1: $L_B$	3: 0.3	N: X
10: 10F	3: 3S	2: 2 $L_C$	5: 0.5 $L_B$	7: 0.7	E: ○

**Figure 5.** Lateral load and displacement relationships (5F1S series).**Figure 6.** Lateral load and displacement relationships (5F3S series).

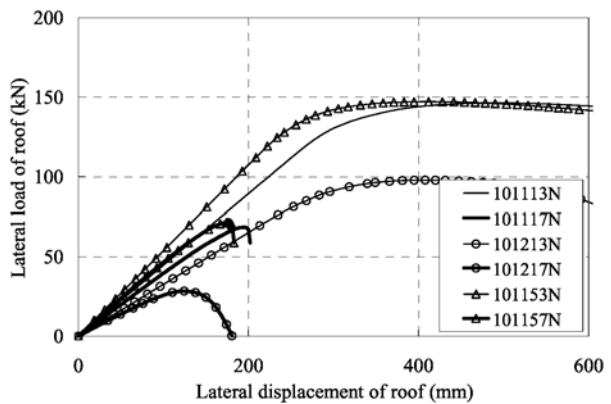
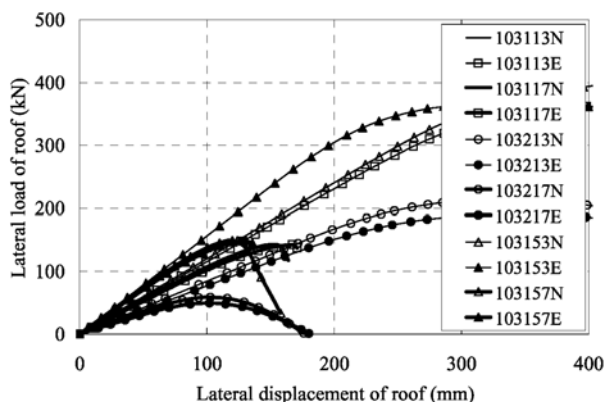
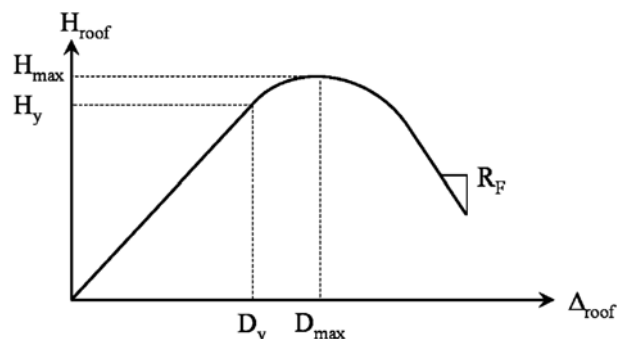
at the first-floor is eliminated, so the length of the right exterior column becomes double. The rule on the case name is summarized in Table 2.

### 2.3. Results of the analysis

The 2-dimensional second-order inelastic analysis was conducted. Most of the analysis results show definite post-maximum load behavior (under  $0.8H_{\max}$ ) but the results do not show enough post-maximum load behavior in some cases of a high axial load ratio or a void. All the results, however, show a peak load.

The lateral load and lateral displacement relationships at the roof level are shown in Figures 5 to 8, and the results related to the lateral load and the lateral displacement relationships are shown in Table 3, and the stiffness related items are shown in Table 4.

In Table 3,  $H_{\max}$  is the maximum lateral load of the roof and  $D_{\max}$  is the lateral displacement of the roof at  $H_{\max}$ .

**Figure 7.** Lateral load and displacement relationships (10F1S series).**Figure 8.** Lateral load and displacement relationships (10F3S series).**Figure 9.** Concepts of the results.

$H_y$  is the lateral load of the roof at the divergent point where the nonlinear behavior started, and  $D_y$  is the lateral displacement of the roof at that time.  $D_{\max}$  and  $D_y$  are the lateral displacements of the first-floor.

In Table 4,  $I_s$  is the initial stiffness of the first-floor, which is defined in Eq. (1).  $S_F(H_y)$  is defined as the index of the lateral resisting capacity of the story in the linear range. It was calculated using Eq. (2) (LeMessurier, 1972).

$R_F$  is the lateral load decrement ratio of the end of analysis ( $\Delta H/\Delta D$ ). The concepts of the abovementioned results are shown in Figure 9.

**Table 3.** Results of the analysis: lateral load and displacement related items

Case	H <sub>max</sub> (kN)	D <sub>max</sub> (mm)	H <sub>y</sub> (kN)	D <sub>y</sub> (mm)	D <sub>max1</sub> (mm)	D <sub>y1</sub> (mm)
51113N	187	292	157	162	75	28
51117N	80	112	50	57	34	10
51213N	99	255	82	160	157	81
51217N	25	77	20	49	49	28
51153N	190	228	156	113	63	20
51157N	85	84	67	69	28	12
53113N	457	279	335	133	92	25
53113E	386	254	285	125	88	26
53117N	166	90	116	51	31	10
53117E	140	89	95	46	34	11
53213N	202	224	169	137	150	77
53213E	179	242	141	133	170	78
53217N	51	69	41	43	48	27
53217E	42	71	31	40	51	26
53153N	462	226	369	106	84	22
53153E	392	203	318	101	75	24
53157N	174	69	130	40	26	9
53157E	150	70	118	42	30	11
101113N	146	492	128	291	40	20
101117N	70	200	55	142	16	11
101213N	98	408	81	253	165	72
101217N	28	125	22	80	51	25
101153N	147	412	131	249	34	17
101157N	78	186	52	113	16	8
103113N	407	525	328	278	61	22
103113E	363	422	303	267	74	26
103117N	143	152	110	103	13	9
103117E	143	167	106	104	22	11
103213N	213	330	177	213	155	71
103213E	191	340	152	203	175	76
103217N	59	103	46	66	49	25
103217E	49	102	37	60	55	25
103153N	405	516	332	282	52	18
103153E	366	333	291	189	65	20
103157N	149	120	105	72	11	6
103157E	149	129	111	81	17	9

$$I_s = (\Sigma H) / D_{y1} \quad (1)$$

where  $\Sigma H$ : the summation of the lateral load at  $H_y$ .

$$S_F(H_y) = \frac{\Sigma H + ((\Sigma P \cdot D_{y1}) / h)}{D_{y1}} \quad (2)$$

where  $P$ : the axial load and  $h$ : the column length.

### 3. The P-δ Effect of the Unbraced Frames

The results of analysis were investigated to get the suitable results for the objectives of this study. For these purpose, there are two groups of investigations. The first

**Table 4.** Results of the analysis: stiffness related items

Case	5 story			10 story		
	I <sub>S</sub> (kN/mm)	S <sub>F</sub> (H <sub>y</sub> ) (kN/mm)	R <sub>F</sub> (kN/mm)	I <sub>S</sub> (kN/mm)	S <sub>F</sub> (H <sub>y</sub> ) (kN/mm)	R <sub>F</sub> (kN/mm)
1113N	21.28	22.49	0.17	56.56	59.12	0.06
1117N	18.29	21.13	1.93	45.15	51.14	-
1213N	3.76	4.36	0.19	9.87	11.15	0.22
1217N	2.66	4.08	0.45	7.43	10.42	1.08
1153N	28.52	29.73	0.16	68.16	70.72	0.08
1157N	21.86	24.70	1.07	58.51	64.49	-
3113N	50.38	52.82	0.32	129.6	134.7	0.15
3113E	40.33	42.76	0.32	101.1	106.3	-
3117N	42.06	47.75	2.79	112.1	124.1	-
3117E	33.35	39.03	2.13	84.25	96.23	-
3213N	8.28	9.49	0.36	21.67	24.23	0.37
3213E	6.75	7.97	0.32	17.59	20.15	0.34
3217N	5.75	8.58	0.85	16.19	22.17	1.32
3217E	4.51	7.34	0.69	12.82	18.80	1.06
3153N	63.28	65.71	0.53	165.3	170.4	-
3153E	49.69	52.12	0.31	129.8	134.9	-
3157N	52.47	58.15	2.11	145.7	157.7	3.79
3157E	38.58	44.26	1.73	109.1	121.0	-

one is about the influence of the P-Δ effect on the behavior of middle-rise unbraced steel frames and the main factors which affect the P-Δ effect. The second one is about the design analysis method, factor B2.

### 3.1. Influence of the P-Δ effect

#### 3.1.1. P-Δ moment

The P-Δ effect induces the additional moment, so called the P-Δ moment and it seriously affect the behavior of unbraced frames (Galambos, 1968, 1998). Thus, it is important to understand the P-Δ moment to design the unbraced steel frames.

In this study, the P-Δ moment ( $M_{pd}$ ) is defined as the additional second-order moment of a specific story induced by the axial load and the lateral displacement. It was calculated using Eq. (3). The first-floor was selected as the target floor to evaluate the P-Δ moment, because the behavior of the first-floor seriously affects the stability and safety of the whole frame (Kim, 2002, 2009).

$$M_{pd} = ((\Sigma P) / N_C) \times D_{1st} \quad (3)$$

where  $N_C$ : the number of columns in the story and  $D_{1st}$ : the lateral displacement of the first-floor.

The P-Δ moment ( $M_{pd}$ ) of each case was calculated using Eq. (3) at  $H_y$  and  $H_{max}$ , and each result was divided by the plastic moment of the beam ( $M_{pb}$ ). The average values of results are plotted in Figure 10 to investigate the effect of the member stiffness, and are plotted in Figure 11 to investigate the effect of the axial load ratio.

The case name of Figure 10 means span,  $L_C$ ,  $L_B$ , and

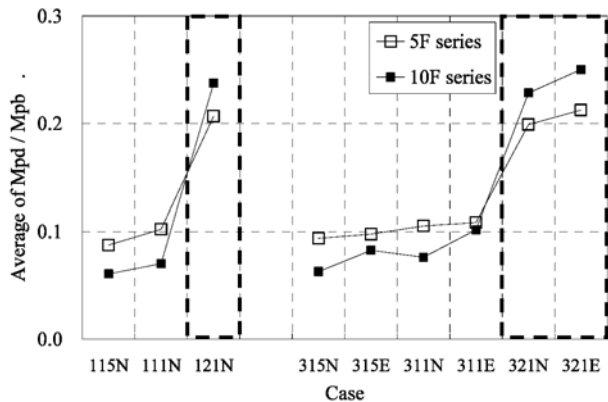


**Figure 10.** Influence of the member stiffness on the average  $M_{pd}/M_{pb}$ .

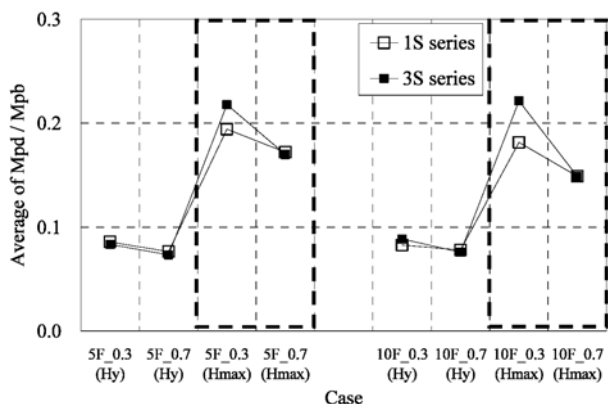
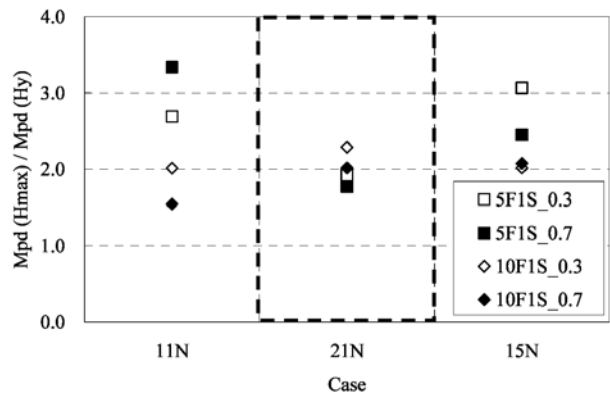


**Figure 11.** Influence of the axial load ratio on the average  $M_{pd}/M_{pb}$ .

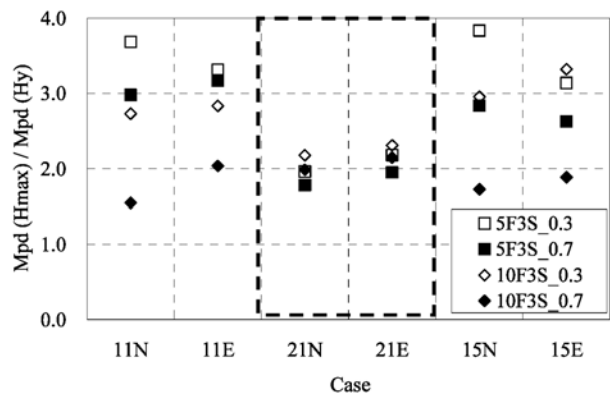
void, and that of Figure 11 means the story and the axial load ratio.

Figure 10 shows that the weak member stiffness cases had high  $M_{pd}$  ratios and those of the 10F series are higher than those of the 5F series in the double-column-length cases (121N, 321N, and 321E). The weak stiffness of the first-floor column may cause the increment of the lateral displacement of the first-floor from the initial loading stage, and it may increase the effect of the P-Δ moment on the first-floor. The lateral displacements of the first-floor,  $D_{y1}$  and  $D_{max1}$ , in Table 3 clearly show this tendency. In this case, the quantity of  $P$ , which is another key of the P-Δ effect, has a greater effect on the P-Δ moment, so the 10F series had a greater P-Δ moment. For the same reason, the E series, the void case, also had a greater P-Δ moment than the N series.

Figure 11 shows that the low axial load ratio cases have higher  $M_{pd}$  ratios and the gap is increased at  $H_{max}$ . This tendency can be explained as follows. A high axial load ratio may cause the yielding of the members from the early stage of loading and a small displacement can cause a P-Δ moment. These effects may accelerate the failure of the frame and sudden failure of the frame can limit the development of lateral displacement. Thus, the lateral displacement decreases (See  $D_{max1}$ ) and the P-Δ moment



**Figure 12.** Ratio of  $M_{pd}(H_{max})$  and  $M_{pd}(H_y)$  (1S series).



**Figure 13.** Ratio of  $M_{pd}(H_{max})$  and  $M_{pd}(H_y)$  (3S series).

cannot increase as much as the axial load ratio. There is very rare possibility of sudden failure in low axial load ratio cases, so displacement can be developed and it causes a high P-Δ moment at an inelastic range.

Thus, the P-Δ effect has to be carefully considered even in low axial load cases if the inelastic behavior is considered in the design. The effect of the number of spans is not serious at  $H_y$  cases, but the three-span cases have higher P-Δ moments in the low axial load at the  $H_{max}$  cases. This tendency is related to above mentioned reason (See  $D_{max1}$ ).

The ratio of the P-Δ moments at  $H_{max}$  and  $H_y$  are plotted in Figures 12 and 13 to investigate the influence of the nonlinear-inelastic behavior on the P-Δ moment. The case name of these figures means  $L_C$ ,  $L_B$ , and void. The increment of the ratio means the effect of the nonlinear-inelastic behavior increases within the P-Δ moment.

These figures show that the ratio increases when the axial load ratio is small. As mentioned above, a low axial load allows inelastic lateral displacement and can produce the P-Δ moment at inelastic range.

In case of the stiffness of the column, the gap between the ratios of the parameters is not noticeable in the weak column stiffness cases (21N and 21E). This phenomenon may be due to the following reason. The weak column governs the behavior of frame from the initial loading

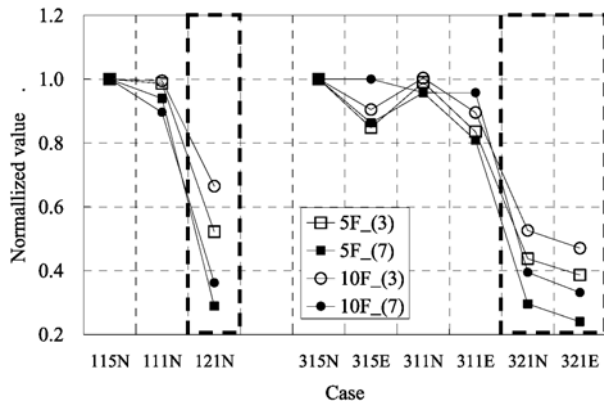


**Figure 14.** Influence of the member stiffness on  $H_{\max}$ .

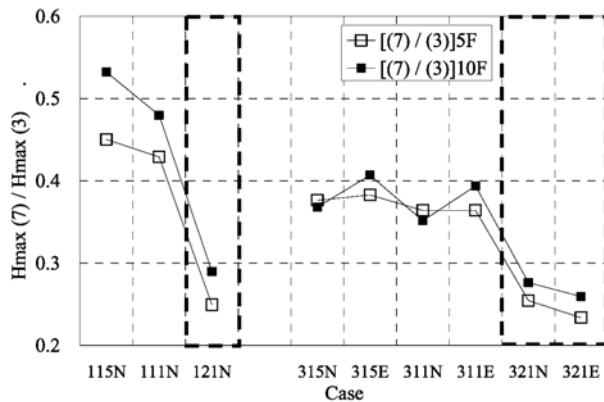


**Figure 15.** Influence of the axial load ratio on  $H_{\max}$ .

stage and it limits the effects of the other parameters. The ratio slightly increases in the high axial load quantity cases in the 10F series.

### 3.1.2. Lateral load and lateral displacement relationships

The relationships between lateral load and lateral displacement are one of important design factors in the serviceability aspect. The P- $\Delta$  effect induces the additional moment and it can increase the lateral displacement. Thus, the P- $\Delta$  effect influences the lateral load and displacement relationships of frames (Kim, 2002, 2009). The maximum lateral load ( $H_{\max}$ ) and the lateral displacement at that time ( $D_{\max}$ ) are summarized in Table 3.

In Figure 14, each  $H_{\max}$  is normalized by the  $H_{\max}$  of each 15N case and it arranged following the order of the beam or the column member's stiffness. The case name means span,  $L_C$ ,  $L_B$ , and void. According to the figure 14, the increment of  $H_{\max}$  is closely related to the stiffness of the frame and the reduction of the first-floor column's stiffness (121N, 321N, and 321E) causes the serious decrement of  $H_{\max}$  in this study.

This trendline is not changed by the variation of the number of spans, the scale of the frame, and the axial load ratio. This phenomenon is also related to the P- $\Delta$  effect. As mentioned before, the weak stiffness member causes a greater P- $\Delta$  effect and this can accelerate the

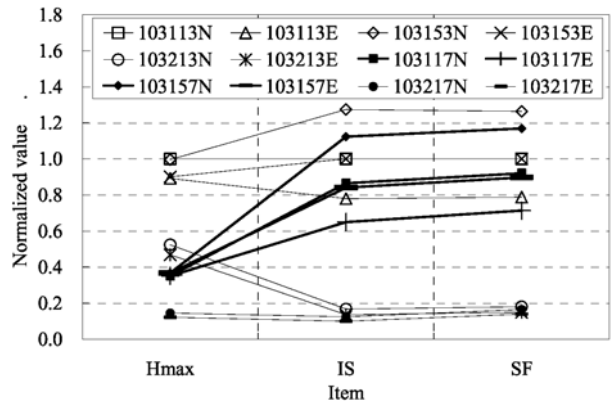


**Figure 16.** Influence of  $I_S$  and  $S_F(H_y)$  on  $H_{\max}$ .

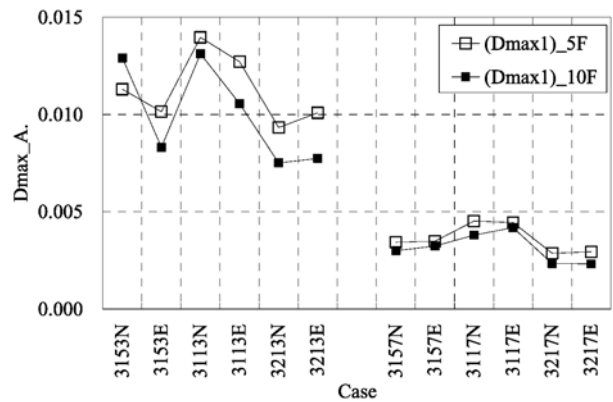


**Figure 17.** Variation in  $D_{\max 1}$ .

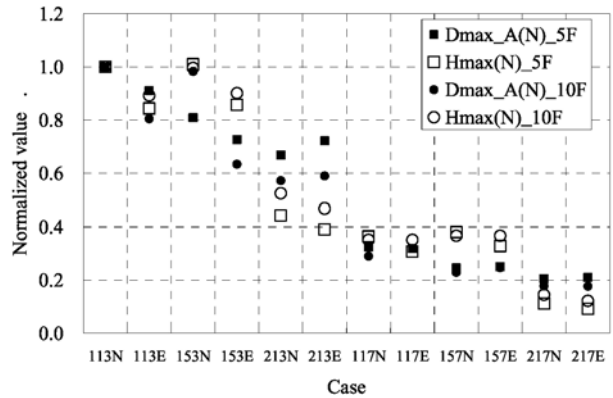


**Figure 18.** Normalized values of  $D_{\max 1}$  and  $H_{\max}$ .

failure of the frame.

The ratios of  $H_{\max}$  between the axial load ratio 0.7 and 0.3 are shown in Figure 15 to investigate the influence of the axial load ratio of the first-floor column on  $H_{\max}$ . The figure shows that the high axial load ratio of the first-floor column could have seriously reduced  $H_{\max}$ .

The reduction in  $H_{\max}$  is especially severe in the double column length cases (121N, 321N, and 321E).

The normalized value of  $H_{\max}$ , the initial stiffness ( $I_S$ ), and the story stiffness [ $S_F(H_y)$ ] of the first-floor in the case of 10F3S series are plotted in Figure 16 to investigate the effect of the frame stiffness on  $H_{\max}$ .

The high  $I_S$  or  $S_F$  case has a high  $H_{max}$  value in most of the low axial load ratio and the weak member stiffness cases.  $I_S$  or  $S_F$  does not estimate  $H_{max}$  properly, however, in case of the sound member stiffness with a high axial load ratio, such as 3117N, 3157N, 3117E, and 3157E. In these cases,  $I_S$  or  $S_F$  of the initial loading stage may be high because the stiffness of the member is sound. However, the P- $\Delta$  moment starts to increase when the lateral displacement is developed. Thus, a sudden failure of the member can occur due to a high axial load and P- $\Delta$  moment, and it may cause a serious reduction in  $H_{max}$  (See Figures 7, 8, 12, and 13).

$D_{max}$  was adjusted using Eq. (4) to consider the difference of the total height of the frame.

$$D_{max\_A} = D_{max}/h_T \quad (4)$$

where  $h_T$ : the total height of the frame.

The values of  $D_{max\_A}$  in the case of the 3S series are plotted in Figure 17. The figure shows that the high axial load ratio of the first-floor column and the high stiffness of the beam may reduce  $D_{max\_A}$ . In the case of a high axial load ratio, it causes the failure of the member with the P- $\Delta$  moment with relatively small lateral displacement. Thus,  $D_{max\_A}$  is reduced. In the case of a high stiffness of the beam, the stiffness of the beam prevents the deformation of the column, so it causes the reduction in  $D_{max\_A}$ . The normalized values of  $D_{max\_A}$  and  $H_{max}$  are shown in Figure 18, and the case name means  $L_C$ ,  $L_B$ , the axial load ratio, and the void. It shows that the trendline of the two items' variations are similar.

To investigate the effect of the nonlinear-inelastic behavior of the frame, the nonlinear-inelastic index ( $I_E$ ) was calculated using Eq. (5).

$$I_E = [(D_{max} - D_y)/h_T] \cdot 100 \quad (5)$$

The increment of this index means that the global behavior, such as the lateral displacement of the frame falls more under the nonlinear-inelastic behavior. The results of the calculations are shown in Figure 19.  $I_E$  has a small value when the axial load ratio of the first-floor column is high because a high axial load accelerates the failure of the member without lateral displacement. In this case, it is hard to develop inelastic lateral displacement.

In case of a weak stiffness of the first-floor column, the softening of the frame condenses in the first-floor from the initial loading stage, so the elastic displacement causes a serious P- $\Delta$  moment. Thus, the global inelastic deformation is limited. Therefore, the proper consideration of the member stiffness and the axial load ratio is very important to achieve ductile and stable frame behavior.

The lateral load reduction ratios are summarized in Table 4. These ratios are closely related to the collapse mechanism of the frame. A high load reduction ratio means that the possibility of the sudden collapse of the frame is high.

The normalized  $S_F$  ( $H_y$ ) and  $R_F$  values in case of 5F3S are plotted in Figure 20 to investigate the effect of the

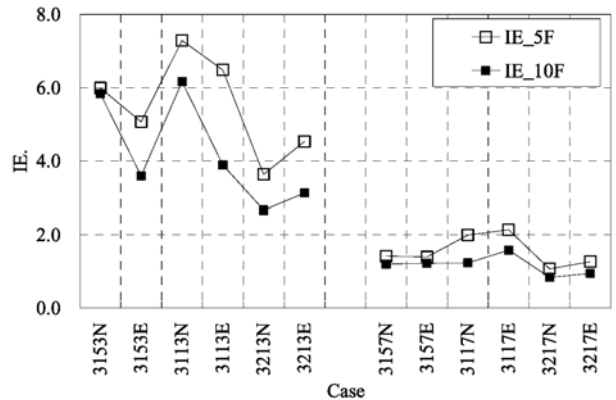


Figure 19. Nonlinear-inelastic index (3S series).

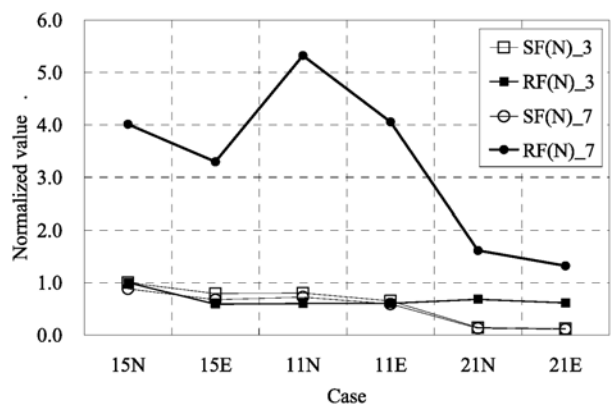


Figure 20. Lateral load reduction ratio (5F3S series).

story stiffness and the axial load ratio. The case name means  $L_C$ ,  $L_B$ , and void. The figure shows that there is no noticeable change in  $R_F$  in case of a low axial load ratio [ $R_F(N)_3$ ], despite a change in the stiffness. The dramatic increment occurs, however, in case of a high axial load ratio [ $R_F(N)_7$ ]. Especially the strong column stiffness cases (11N) have high  $R_F$  values. Thus, the main factor that controls the post-maximum load behavior of the unbraced frame is the axial load ratio.

After the maximum load, the frame structure seriously softened. Thus, the influence of the P- $\Delta$  effect on the stability of the frame is fully governed by the axial load.

### 3.1.3. Story stiffness

The P- $\Delta$  effect is directly affected by the lateral displacement of story ( $\Delta$ ) and it is closely related to the stiffness of frame. Story stiffness is the index which shows the lateral stiffness of certain story. In addition, the linear-elastic story stiffness is the basis of factor B2.

The story stiffness has a constant value when the structural behavior stays in the linear-elastic range but starts to decrease when structural softening, such as the yielding of the material, is started (Kim, 2002, 2009).

The story stiffness values of all the cases at  $H_y$  are summarized in Table 4. The ratio of  $S_F(H_{max})$  to  $S_F(H_y)$  of 5F series is shown in Figure 21 to evaluate the

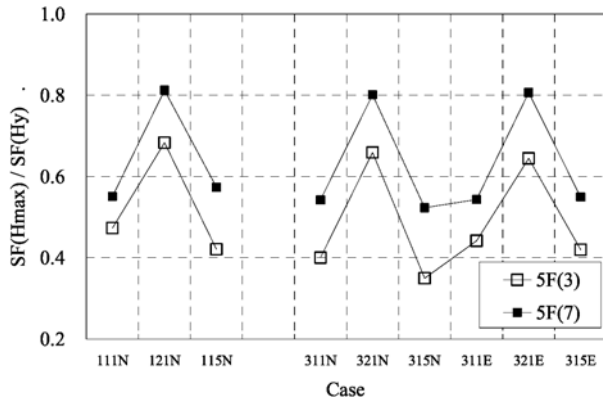
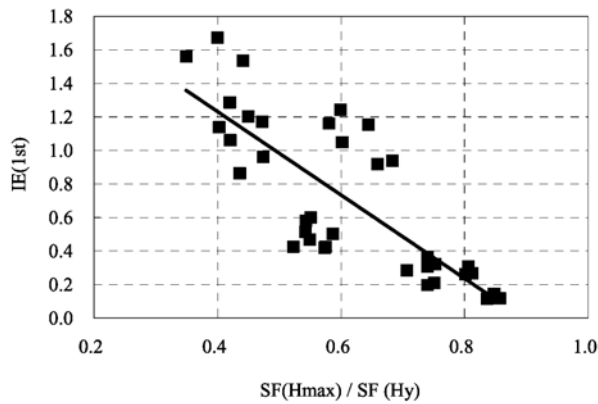
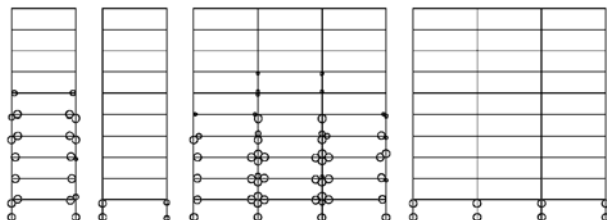
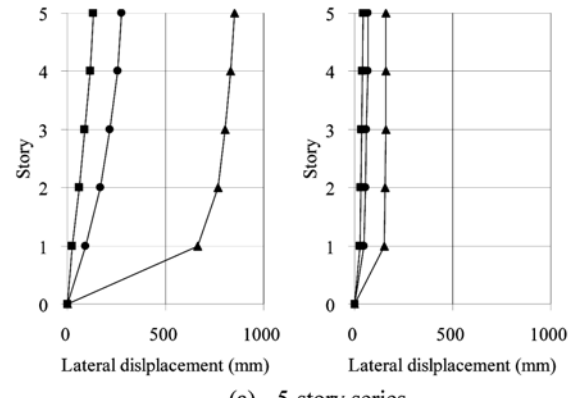
Figure 21.  $S_F$  ratio of  $H_{\max}$  to  $H_y$ .Figure 22. Influence of  $I_E$  on the  $S_F$  ratio.

Figure 23. Plastic hinge development (Left: 113N, Right: 217N).

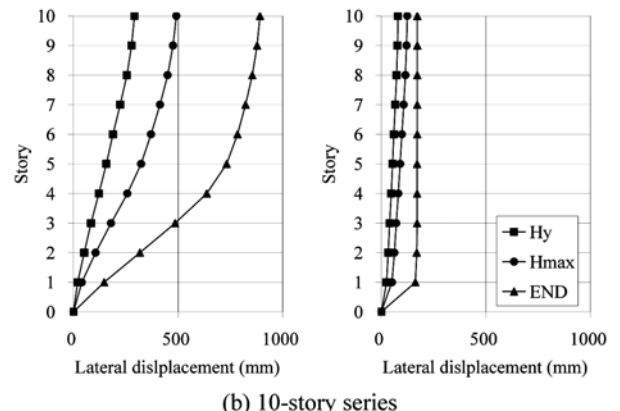
variation in the  $S_F$  value. The case name means span,  $L_C$ ,  $L_B$ , and void. The figure shows that the story stiffness decreases when the load reaches its maximum value.

The reduction in  $S_F$  is related to  $I_E$ . The high  $I_E$  cases with low axial load ratio, such as the 11 ( $L_C$  and  $L_B$ ) and 15 ( $L_C$  and  $0.5L_B$ ) series had noticeable reductions in  $S_F$  (See Figures 19 and 21). The relationship between  $I_E$  at the first-floor and the ratio of  $S_F$  is shown in Figure 22 to look into the common relationships between the two subjects. In this figure, the high  $I_E$  value causes a big gap between  $S_F(H_y)$  and  $S_F(H_{\max})$ .

The reduction in  $S_F$  starts when the nonlinear-inelastic behavior is induced. Therefore, factor B2, which is based on the linear-elastic  $S_F$ , cannot properly estimate the moment amplification effect when the nonlinear-inelastic behavior of the frame is started. Therefore, the variation in  $S_F$  is properly considered.



(a) 5-story series



(b) 10-story series

Figure 24. Deformed shape at  $H_y$ ,  $H_{\max}$ , and the end of the analysis (Left: 113N, Right: 217N).

### 3.1.4. Collapse mechanism

After the maximum load, the increment of lateral displacement is accelerated. In that case, the influence of the P- $\Delta$  effect also increases (Kim, 2002, 2009). Thus, it is meaningful to investigate the collapse mechanism to understand the P- $\Delta$  effect and the behavior of unbraced frames at the inelastic range.

The plastic hinge locations after the maximum lateral load were investigated. The results of the ten-story structure's 113N and 217N series ( $L_C$ ,  $L_B$ , axial load ratio, and void) are shown in Figure 23. The plastic hinges are developed in the beam and column ends and properly distributes in the low axial load and sound stiffness cases, such as the 113N series. The plastic hinges are developed in the column ends, however, and their location is limited to the first-floor in the high axial load or weak column stiffness cases, such as the 217N series. This result is easily expected throughout the previous investigation results.

The lateral displacements of all the floors at  $H_y$ ,  $H_{\max}$ , and the end of the analysis are plotted in Figure 24 to investigate the procedure of the collapse mechanism and the deformed shape of frame.

Lateral displacements are distributed well in the low axial load ratio and sound stiffness cases, such as the 113N series. Limited lateral displacement is allowed, however, and the deformation is condensed into the first-floor column in the high axial load and weak column

stiffness cases, such as the 217N series.

As mentioned before, it is closely related to the P- $\Delta$  effect. Thus, proper consideration of the P- $\Delta$  effect is the one of the most important factor for the design of an acceptable collapse mechanism.

In addition, it can be said that the role of the first-floor column's behavior increases in extreme structural conditions.

### 3.2. Validity of factor B2

#### 3.2.1. Factor B2 and the moment amplification factor

In KBC 2009, there are several methods that can consider the second-order effects, such as the P- $\delta$  and P- $\Delta$  effects. Factor B2 is suggested to consider the P- $\Delta$  effects. Therefore, it is very important for structural engineers to understand the validity and the limitation of factor B2 clearly. To understand factor B2, the results of factor B2 were compared with the moment amplification factor which was calculated from the second order inelastic analysis results.

In KBC 2009, two types of equations are suggested for the calculation of factor B2.

$$B_2 = \frac{1}{\sum P_{nt}} \geq 1.0 \quad (6)$$

$$1 - \frac{\sum P_{nt}}{\sum P_{e2}}$$

$$P_{e2} = \sum \frac{\pi^2 EI}{(K_2 h)^2}, \quad (7)$$

$$= 0.85 \frac{\Sigma H h}{\Delta_H}, \quad (8)$$

where  $E$ : the modulus of elasticity of steel;  $I$ : the moment of inertia in the plane of bending;  $K_2$ : the effective length factor in the plane of bending; and  $\Delta_H$ : the first-order inter-story drift due to the lateral forces,

In the design code, the selection of either Eq. (7) or Eq. (8) fully depends on the engineer's discretion. In this study, factor B2 was calculated using both the aforementioned methods. An elastic analysis was conducted to obtain the  $\Delta_H$  values at the elastic range using a commercial analysis program. To obtain a more precise  $K_2$  value, the alignment chart in KBC 2009 was used.

The moment amplification factor of the analysis results ( $A_F$ ) was calculated using Eq. (9) and the results were compared with factor B2.

$$A_F = M_{second}/M_{first} \quad (9)$$

$$M_{second} = \sum (M_U + M_D) \quad (10)$$

$$M_{first} = M_{second} - \sum (P \cdot D_{1st}) \quad (11)$$

where  $M_U$ : the upper moment of the column;  $M_D$ : the bottom moment of the column; and  $D_{1st}$ : the lateral displacement of the first-floor.

The first-floor is the target of the comparison because the P- $\Delta$  effect is maximized at the first-floor and the behavior of the first-floor governs the stability of the

**Table 5.** Factor B2 and  $A_F$  at the first-floor

Case	$A_F$ ( $H_y$ )	$A_F$ ( $H_{max}$ )	B2 [(6), (7)]	B2 [(6), (8)]
51113N	1.057	1.122	1.072	1.067
51117N	1.155	1.323	1.186	1.198
51213N	1.162	1.256	1.320	1.191
51217N	1.534	1.750	2.303	1.734
51153N	1.043	1.107	1.057	1.054
51157N	1.130	1.251	1.145	1.150
53113N	1.048	1.131	1.064	1.058
53113E	1.059	1.144	-	-
53117N	1.135	1.281	1.163	1.167
53117E	1.167	1.346	-	-
53213N	1.147	1.241	1.279	1.173
53213E	1.173	1.294	-	-
53217N	1.495	1.704	2.040	1.643
53217E	1.608	1.881	-	-
53153N	1.038	1.119	1.052	1.048
53153E	1.048	1.122	-	-
53157N	1.108	1.230	1.132	1.136
53157E	1.143	1.279	-	-
101113N	1.045	1.080	1.058	1.058
101117N	1.133	1.161	1.148	1.164
101213N	1.130	1.247	1.249	1.155
101217N	1.404	1.618	1.868	1.541
101153N	1.038	1.067	1.046	1.048
101157N	1.103	1.142	1.114	1.140
103113N	1.039	1.087	1.051	1.049
103113E	1.050	1.118	-	-
103117N	1.106	1.127	1.129	1.144
103117E	1.139	1.208	-	-
103213N	1.118	1.213	1.217	1.139
103213E	1.140	1.256	-	-
103217N	1.370	1.575	1.712	1.474
103217E	1.451	1.721	-	-
103153N	1.031	1.074	1.042	1.042
103153E	1.039	1.103	-	-
103157N	1.082	1.100	1.104	1.126
103157E	1.108	1.150	-	-

frame.  $A_F$  and factor B2 at the first-floor are summarized in Table 5.

It is not possible to calculate factor B2 in cases of void (as in the E series) because there is no concept of story. The average  $A_F$  value in the void cases is 1.177 at  $H_y$  and 1.302 at  $H_{max}$ , though. These values cannot be neglected. Thus, another approach is needed for the void case to consider the P- $\Delta$  effect with factor B2.

The ratio of factor B2, which was calculated using Eqs. (6) and (7), to factor B2, which was calculated using Eqs. (6) and (8), is shown in Figure 25. The case name means  $L_C$ ,  $L_B$ , the axial load ratio, and the void.

The figure shows that there is no considerable difference between the two sets of results in the 11 ( $L_C$

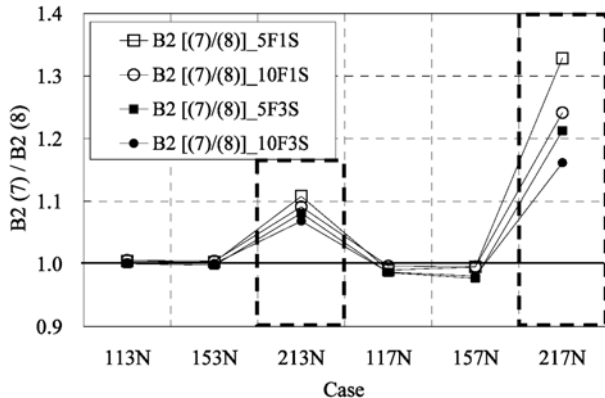


**Figure 25.** Ratio of factor B2 between Eqs. (7) and (8).

and  $L_B$ ) and 15 ( $L_C$  and  $0.5L_B$ ) series, but the gap sharply increases in the weak column stiffness cases, such as the 21 (2 $L_C$  and  $L_B$ ) series and high axial load amplifies the gap between the two methods.

In this study, factor B2 which was calculated using Eqs. (6) and (7), the story-buckling concept tended to yield a high value. Thus, it is important to select the equation of factor B2 when factor B2 is applied on a frame with weak column stiffness.

### 3.2.2. Verification of factor B2

The results of factor B2, which were calculated with Eqs. (7) and (8), were divided by the  $A_F$  from the analysis results to verify the validity of factor B2. The results are plotted in Figures 26 and 27.

In these figures, factor B2 reasonably estimate P- $\Delta$  effect in the linear-elastic range (the  $H_y$  cases), but the factor B2 that was calculated using Eq. (7) overestimates the P- $\Delta$  effect in the weak column stiffness with high axial load ratio cases, such as the 217N series.

It may not cause a safety problem to overestimate the P- $\Delta$  effect from the single-member level. It is not a safe and economic way of design, however, from the overall structural perspective.

Thus, reasonable guidelines are needed for the selection of the equation to be used for the calculation of factor B2, because the reliability of the equation is affected by the structural conditions.

From these points of view, factor B2, using the story stiffness concept, produces more reasonable results in the linear-elastic range regardless of the stiffness of the column or the axial load ratio in this study.

The moment amplification factor sharply increased, however, when the frame behavior loses its linear elasticity. The factor B2 suggested in KBC 2009, however, has a constant value regardless of the frame conditions. Thus, factor B2 underestimates the P- $\Delta$  effect when the frame behavior loses its linear elasticity. Figures 26 and 27 show this problem. Except for some weak column stiffness cases, all the others underestimate the P- $\Delta$  effect.

This is a totally different problem compared with

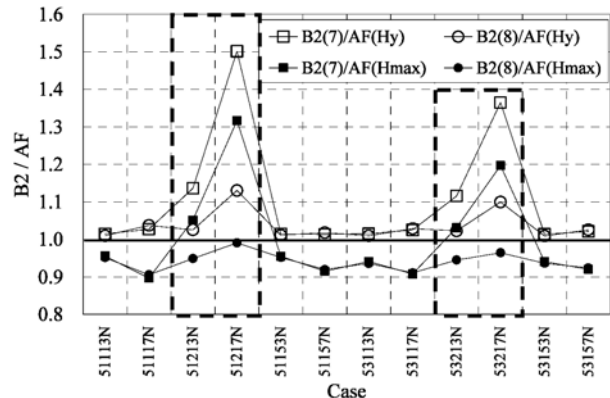


**Figure 26.** Ratio of factor B2 to  $A_F$  (5F series).

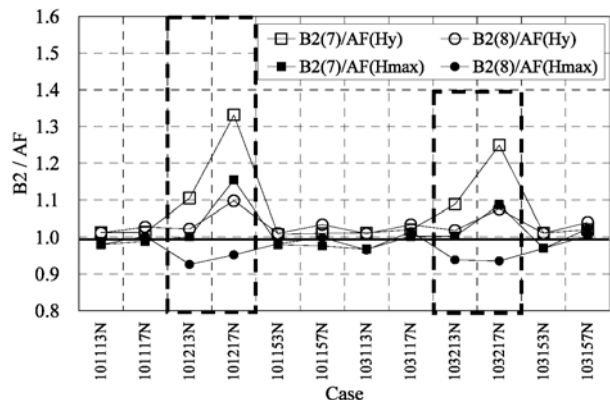


**Figure 27.** Ratio of factor B2 to  $A_F$  (10F series).

overestimation. Thus, it can be said that factor B2 is no longer valid when the frame behavior loses its linear elasticity. KBC 2009 is based on the limits state design, so it allows the use of the inelastic range of the material strength in the member design. Thus, further investigation is needed to suggest clear limits in the use of factor B2.

## 4. Summary and Conclusion

The results of this study can be summarized as follows.

The behavior of unbraced steel frames, such as their maximum lateral load, lateral displacement, nonlinear-inelastic behavior, story stiffness decrement, and collapse mechanism, are affected by the P- $\Delta$  effect.

The influence of the P- $\Delta$  effect is highly affected by the axial load and the stiffness of the first-floor column, and the P- $\Delta$  moment can be increased under the conditions that allow an inelastic displacement even in a low axial load case. The axial load becomes the main factor that governs the behavior of the frame after the maximum load is applied.

In some cases, the selection of equation for the computation of factor B2 can make the result different. The difference between the equations increases in a case with a weak column stiffness and a high axial load. In this study, factor B2, which is based on the story stiffness

concept, yielded a reasonable result in the linear-elastic region. Factor B2 is not applicable, however, to the frame that has not clear story concept and it underestimates the P- $\Delta$  effect when the nonlinear-inelastic behavior starts to be induced. Thus, it is recommended to use Factor B2, which is based on the story stiffness concept, when the unbraced steel frame, which has clear story concept, is designed in the elastic range. If the frame is not suitable for above mentioned conditions, the careful consideration is needed for the use of factor B2.

## References

- AIK (2009). *Korean building code for structures*. Architectural Institute of Korea (in Korean).
- Chan, S. L. and Zhou, Z. H. (2000). "Non-linear integrated design and analysis of skeletal structures by 1 element per member." *Engineering Structures*, 22(3), pp. 246-257.
- Chen, W. F. and Chan, S. L. (1995). "Second-order inelastic analysis of steel frames using element with midspan and end spring." *Journal of Structural Engineering*, ASCE, 121(3), pp. 530-541.
- Chen, W. F. and Lui, E. M. (1991). *Stability design of steel frames*. CRC Press, USA.
- Chen, W. F. and Sohal, I. (1995). *Plastic design and second-order analysis of steel frames*. Springer-Verlag, USA.
- Cheong-Siat-Moy, F. (1972). "Consideration of secondary effects in frame design." *Journal of Stru. Div. ASCE*, 103(ST10), pp. 2005-2019.
- Crisfield, M. A. (1983). "An Arc length method that includes line searches and accelerations." *International Journal for Numerical Methods in Engineering*, 19(9), pp. 1269-1289.
- Galambos, T. V. (1968). *Structural members and frames*. Prentice Hall, USA.
- Galambos, T. V. (1998). *Guide to the stability design criteria for metal structures, 5<sup>th</sup> Edition*. John Wiley & Sons, Inc., USA.
- Kim, H. D. and Lee, M. J. (2001). "An experimental study on the P- $\Delta$  influence of weak-beam unbraced frames." *Journal of the Korean Society of Steel Construction*, 13(4), pp. 363-372 (in Korean).
- Kim, H. D. and Lee, M. J. (2002). "The influence of the P- $\Delta$  effects on the behavior of unbraced frames." *Proc. ISSS 2002*. KSSC, Korea, pp. 333-344.
- Kim, H. D. (2002). *P- $\Delta$  Effects in the case of unbraced steel frames*. Doctoral dissertation, Chungang University, Korea (in Korean).
- Kim, H. D. and Lee, M. J. (2009). "Experimental investigation of the P- $\Delta$  effect and factor B2 of low-rise unbraced steel frames." *International Journal of Steel Structures*, 9(2), pp. 131-141.
- Kim, S. E. and Chen, W. F. (1998). *LRFD steel design using advanced analysis*. CRC Press, USA.
- Kim, T. J. and Jo, J. S. (2007). *Design manual for low-rise steel buildings*. Hyundai Steel, Korea.
- LeMessurier, W. J. (1972). "A practical method of second-order analysis (Part 2: Rigid Frames)." *Engineering Journal*, AISc, 14(2), pp. 89-96.
- Moon, K. S. and Ali, M. M. (2007). "Structural developments in tall buildings: current trends and future prospects." *Architectural Science Review*, University of Sydney, 50(3), pp. 205-223.
- Yura, J. A. (1971). "The effective length of columns in unbraced frames." *Engineering Journal*, AISc, 8(2), pp. 37-42.